



ELSEVIER

Journal of Photochemistry and Photobiology A: Chemistry 142 (2001) 151–161

Journal of
Photochemistry
and
Photobiology
A: Chemistry

www.elsevier.com/locate/jphotochem

Photoinduced electron transfer in non-aqueous microemulsions

Sílvia M.B. Costa*, Pilar López-Cornejo¹, Denisio M. Togashi, César A.T. Laia*Centro de Química Estrutural, Complexo I, Instituto Superior Técnico, Av. Rovisco Pais, 1049-001 Lisboa Codex, Portugal*

Dedicated to Professor Lord Porter, O.M., F.R.S.

Abstract

Photoinduced electron transfer from zinc tetraphenyl porphyrin (ZnTPP) incorporated in *n*-heptane/AOT/ethylene glycol microemulsions was followed by laser flash photolysis and fluorescence quenching. Using two acceptors, duroquinone (DQ) and methyl viologen (MV²⁺) which are located on opposite sides of the interfacial region, the apolar and polar pseudophases respectively, it was possible to monitor kinetic and spectroscopically the respective radical ions formed. The determination of local quencher concentrations enabled the evaluation of electron transfer quenching rate constants in each pseudophase. The values obtained showed that when both the fluorophore and the quencher are either in the oil pseudophase or at the interface the processes are diffusion-controlled limited. The magnitude of the rate constants ranges from 10⁸ to 10¹⁰ mol⁻¹ dm³ s⁻¹. By contrast, the forward electron transfer occurring in the polar pool is reaction controlled ($k_q^T = 2.1 \times 10^6$ mol⁻¹ dm³ s⁻¹) whereas the back recombination of radical ions in the pool is also diffusion controlled ($k_2 = 4.1 \times 10^8$ mol⁻¹ dm³ s⁻¹).

The triplet state kinetics is well supported by steady-state and transient fluorescence quenching studies from which effective reactional distances (9–12 Å) and diffusion coefficients (0.5–1.3) × 10⁻⁹ m² s⁻¹, could be evaluated at both the oil and interface pseudophases. The larger effective reaction distances coupled with lower diffusion coefficients estimated at the interfacial region connected to the polar non-aqueous solvent shows that factors such as the distance, mutual orientation and microviscosity are the controlling physical parameters. On the other hand, beyond the energetics, the efficiency of the whole electron transfer in the inner polar non-aqueous nanophase depends on the solvation of radical ions formed. © 2001 Elsevier Science B.V. All rights reserved.

Keywords: Microemulsions; Zinc tetraphenyl porphyrin; Duroquinone; Methyl viologen; Electron transfer

1. Introduction

Molecular aggregates, such as micelles, vesicles and microemulsions, have been widely used as model systems to mimic some of the various functions of biological organizations [1].

Microemulsions are apparently homogeneous and stable thermodynamical systems, which are formed by a mixture of apolar and polar solvents, stabilised by amphiphilic molecules called surfactants [2]. The aggregation occurs in the following manner: the aliphatic tails of the surfactant molecules extend into the organic pseudophase, the polar headgroups and the counterions reside in the inner core where they are solvated by the polar solvent molecules. The majority of the studies on microemulsions have used water as the polar component [3–5]. Several reports, however, appeared in the literature where water was substituted by a

polar non aqueous solvent [6–8]. The pool size of aggregates is controlled by the polar solvent-to-surfactant molar ratio [polar solvent]/[surfactant] and is independent either on the nature of the non-polar solvent or on the surfactant concentration [9–12]. The aggregate structure of these microemulsions with polar non-aqueous pools of glycerol (Gly), ethylene glycol (Et Gly) and formamide (Form) was recently investigated by dynamic and static light scattering techniques [13,14]. Solvation dynamics in restricted environments were also studied by femtosecond spectroscopy incorporating fluorescence probes, coumarin dyes, in these microemulsions [15]. Nevertheless, very few photophysical studies are known in these systems and, as regards photochemical reactions, it is likely that the diffusion of reactants in the media is affected by its distribution at the interface.

Fluorescence quenching associated to photoinduced electron transfer has been studied extensively in molecular organizations such as reverse micelles and microemulsions [16–19]. Different redox pairs have been investigated, but during the last decade several studies of linked porphyrin–quinone systems have been conducted to

* Corresponding author. Tel.: +351-218419000; fax: +351-218464455.

E-mail address: sbcosta@popsrv.ist.utl.pt (S.M.B. Costa).

¹ Permanent address: Departamento de Química Física, Facultad de Química, Universidad de Sevilla, 41012 Sevilla, Spain.

mimic chlorophyll donors and quinone acceptors in natural photosynthesis [20–22].

Recently, the photophysical properties of zinc tetraphenylporphyrin (ZnTPP) were studied in *iso*-octane (*n*-heptane)/AOT/Et Gly microemulsions [23]. Results of steady state and transient fluorescence revealed the existence of two spectroscopic ZnTPP species located at different environments of the reverse micelles. The presence of ethylene glycol in the medium produces a displacement of porphyrin molecules, from the organic bulk to the location of the polar solvent, which is situated close to the interface. This displacement was explained by considering the existence of a specific interaction between the ethylene glycol and the porphyrin's Zn metal coordinated ion, which could also be related to the probe solvation by ethylene glycol. The partition effect can also be observed with ZnTMPyP⁴⁺ in AOT aqueous microemulsions as shown recently by steady-state and transient absorption data [24] since this water soluble porphyrin which is located in the vicinity of the negatively charged interface can probe hydrophilic and hydrophobic regions. By contrast, the neutral ZnTPP incorporated in the non aqueous microemulsions resides in the apolar organic phase in aqueous AOT microemulsions and the use of this probe for quenching studies, in this very well known system, restricts this phenomena essentially to the oil pseudo-phase where confinement effects are not felt.

In the present work, we report the fluorescence quenching of the electron donor (ZnTPP) by one electron acceptor, duroquinone (tetramethyl-1,4-benzoquinone, DQ) [17]. The ZnTPP triplet state quenching which gives direct evidence of electron transfer [25] was studied using two acceptors. Besides duroquinone, which resides essentially in the organic pseudo-phase (*n*-heptane), the other acceptor is methyl viologen (MV²⁺), which locates exclusively in the inner core of the polar entrapped solvent (ethylene glycol) in non-aqueous microemulsions of sodium 1,4-bis-2-ethylhexyl sulfosuccinate (AOT). In this paper, we aim to present a phenomenological picture of the photoinduced electron transfer with different kinetic features which can occur in these new compartmentalised systems and the interfacial effects on the rate constants.

2. Experimental

2.1. Materials

Sodium 1,4-bis(2-ethylhexyl)sulfosuccinate was purchased from Fluka and purified according to literature [26]. The AOT concentration used was 0.1 mol dm⁻³ for all measurements. The molar ratio, $e_o = [\text{ethyleneglycol}]/[\text{AOT}]$ was altered within the 0–2 range with fixed surfactant concentration. It was not possible to work at $e_o > 2$ due to stability problems of the microemulsions [13]. Zinc tetraphenylporphyrin (Hambright, Washington, DC), Duroquinone (Aldrich) and Methyl Viologen (Sigma) were used without further purification. The concentration of ZnTPP

was always 4×10^{-6} mol dm⁻³. Ethylene glycol (Aldrich, HPLC grade) and *n*-heptane (Aldrich, HPLC grade) were used as received. The water incorporated in the aqueous microemulsions was bidistilled.

2.2. Sample preparation

Singlet state studies used aerated solutions, but in the triplet studies samples were thoroughly degassed with argon before carrying out kinetic measurements or obtaining transient absorption spectra.

2.3. Apparatus

Absorption spectra were recorded with a JASCO V-560 UV/VIS spectrophotometer. Steady-state fluorescence emission spectra were obtained with a Perkin-Elmer LS 50B spectrofluorimeter with the sample holder thermostated at 298 K. The instrumental response at each wavelength was corrected by a curve provided with the apparatus.

The fluorescence decays were measured by the time-correlated Single Photon Counting [27] method using a Photon Technology International LS 100 with the sample holder thermostated also at 298 K. Decay data was analysed by an iterative deconvolution procedure based on the Marquardt algorithm [28]. The lifetime results are an average of decay data made at different excitation and emission wavelengths. The reduced Chi-square (χ^2) and the Durbin Watson parameters (D.W.) were used to test the quality of fitting during the analysis procedure.

The transient absorption spectra and the kinetics of the intermediates in the triplet excited state were recorded by a laser flash photolysis equipment using the second harmonic (532 nm, 65 mJ, 8 ns) of a Nd-YAG laser (Spectra-Physics, System Quanta-Ray GCR-3) as an excitation source. The kinetic spectrometer (10 ns resolution) included an averaging system consisting of a Tektronix 2430A digital oscilloscope coupled to a PDP 11/73 microcomputer. Kinetic curves were averaged over at least 32 laser pulses. Laser flash photolysis data was analysed by a non-linear least squares method using a global lifetime analysis [29]. In the present work, we have analysed the decays in the same medium at different wavelengths and obtained the transient absorption spectra in the range of 380–600 nm. The best fitting parameters were obtained by the minimisation of the sum of the squared differences between the calculated and the experimentally observed variables.

3. Results and discussion

3.1. Absorption spectra of ZnTPP/DQ in *n*-heptane

The absorption spectra of solutions of ZnTPP in *n*-heptane in the presence of different concentrations of DQ were recorded. A slight red shift of the Q bands, as well as a clear

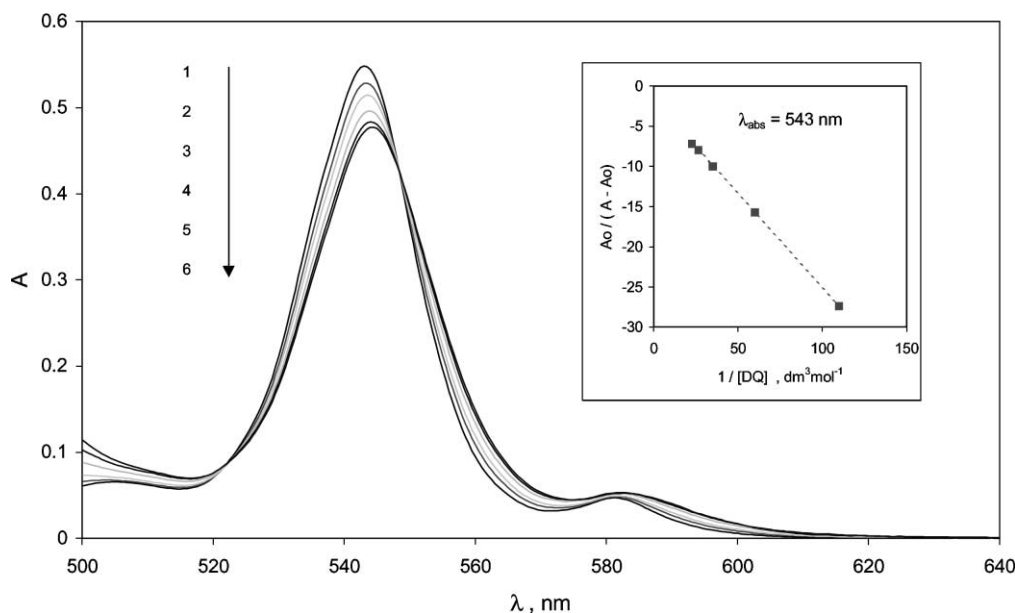


Fig. 1. Absorption spectra of ZnTPP in *n*-heptane with [DQ], M: (1) 0; (2) 9.1×10^{-2} ; (3) 1.7×10^{-2} ; (4) 2.9×10^{-2} ; (5) 3.75×10^{-2} ; and (6) 4.4×10^{-2} . The inset shows the absorption ratio of initial ZnTPP and the free ZnTPP vs. $1/[DQ]$.

isosbestic shift of about 550 nm were obtained (Fig. 1). On the other hand, a decrease of the maximum absorbance in the Q and Soret bands was observed by increasing the quencher concentration,² which confirm an interaction between ZnTPP and DQ in *n*-heptane. The linear correlation of the ratio of absorbance changes with the reciprocal of the duroquinone concentration afforded the association constant in *n*-heptane, $K_c = 7.9 \text{ M}^{-1}$ and the ratio of maxima absorptivities $\varepsilon_f = (\varepsilon_{\text{ZnTPP-DQ}}/\varepsilon_{\text{ZnTPP}}) = 0.45$ (inset of Fig. 1).

3.2. Fluorescence quenching of ZnTPP by DQ in *n*-heptane

The steady-state fluorescence quenching of the ZnTPP by duroquinone shows a pronounced upward curve, which can be associated with the formation of a ground state complex (Fig. 2) [27]. In addition to this factor, the static quenching of fluorophores by the fraction of quenchers that are placed statistically close to the fluorophore may contribute to the positive deviation of the experimental data.

For species with short lifetimes, the so-called transient effects can also contribute to positive deviations in the fluorescence intensity ratios I_f^0/I_f to the fluorescence lifetime ratios (τ_f^0/τ_f) in the presence of a quencher. The term

$$Y = 1 - x\pi^{1/2} e^{x^2} \text{erfc}(x),$$

² The decrease of optical densities in the Soret band was observed after subtracting the absorption spectrum of duroquinone to the absorption spectrum of the ZnTPP + DQ mixture, at the same concentration of quencher and medium, due to the great absorption of duroquinone in that wavelength range.

where

$$\text{erfc}(x) = \frac{1}{2^{1/2}\pi} \int_x^\infty e^{-\xi^2} d\xi,$$

$$x = \frac{b}{a^{1/2}}, \quad a = \frac{1}{\tau_f^0} + 4\pi N'_a D' R' [Q]$$

$$\text{and } b = (2R')^2 (\pi D')^{1/2} N'_a [Q]$$

has to be taken into account enabling the determination of D' which is the sum of diffusion coefficients of both species and R' the distance at which the bimolecular interaction proceeds with unit efficiency.

The steady-state data can be fitted by using a modified Stern–Volmer Eq. (1) [30–33], taking into account the ratio of absorptivities ε_f

$$\frac{I_f^0}{I_f} = (1 + K_{sv} [Q]) (1 + \varepsilon_f K_c [Q]) \exp(N'_a V [Q]) Y^{-1} \quad (1)$$

where K_{sv} is the Stern–Volmer constant ($K_{sv} = k_q \tau_f^0$; k_q the quenching rate constant and τ_f^0 the lifetime of the luminescence species in the absence of quencher), K_c the association constant of the ZnTPP–DQ complex, N'_a the Avogadro number multiplied by 10^{-3} , and $V = (4\pi/3)(R'^3 - R_f^3)$ the quenching volume in cm^3 around the fluorophore, with R_f being the radius of the chromophore and R' is the reaction distance.

The dynamic fraction was determined directly from the linear slope obtained from Eq. (2) of transient data (Fig. 2)

$$\frac{\tau_f^0}{\tau_f} = (1 + k_q \tau_f^0 [Q]) \quad (2)$$

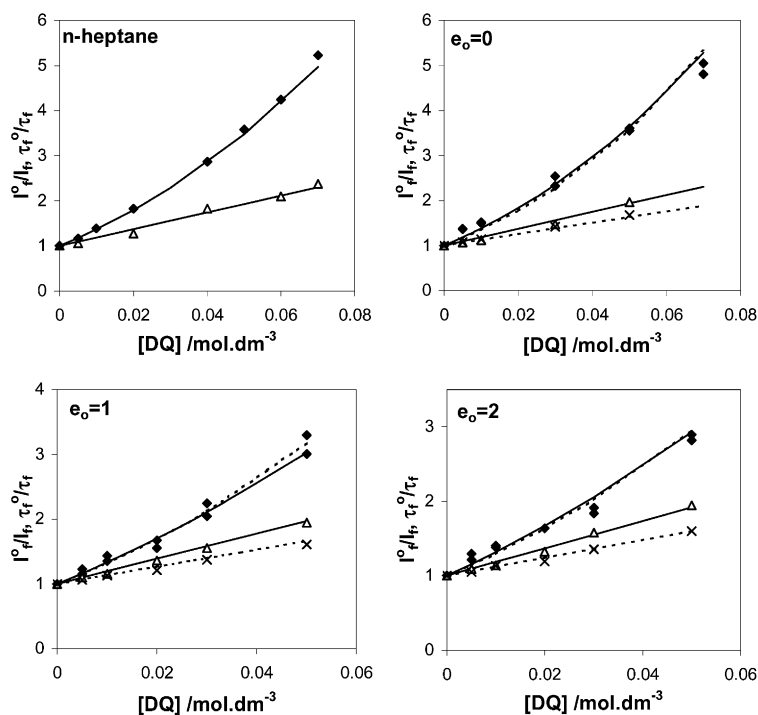


Fig. 2. Fluorescence quenching of ZnTPP by DQ in *n*-heptane: I_f^0/I_f (◆), τ_f^0/τ_f (△) and in *n*-heptane/AOT/ethylene glycol microemulsions at $e_o = 0, 1$ and 2 ; I_f^0/I_f (◆), τ_f^0/τ_f (△, X). Symbols △ and X correspond to the lifetimes of the ZnTPP molecules located at the organic bulk and the interface of the aggregates, respectively. Lines are the best fitting of the experimental results using Eqs. (1) and (2).

Monoexponential decays were observed in pure *n*-heptane up to a concentration of $3.0 \times 10^{-2} \text{ mol dm}^{-3}$ duroquinone. Deviations from exponentiality above this concentration were very small and not taken into consideration.

The k_q rate constant obtained from transient measurements is $9.43 \times 10^9 \text{ mol}^{-1} \text{ dm}^3 \text{ s}^{-1}$ (τ_f being the lifetimes of free ZnTPP molecules in the presence of quencher). The calculated diffusion-controlled rate constant value is $(1.7\text{--}2.1) \times 10^{10} \text{ mol}^{-1} \text{ dm}^3 \text{ s}^{-1}$ and is obtained using the Eq. (3) (the value depends on the radii values used, see later) [34]:

$$k_q^{\text{calc}} = 4\pi RDN_a \quad (3)$$

Here, we have assumed that the radius R is the sum of R_{ZnTPP} and R_{DQ} and that the diffusional coefficient D is equal to $D_{\text{ZnTPP}} + D_{\text{DQ}}$. The radii of the different species were found in literature [35,36] and are in the range 5–8 Å for ZnTPP and 3–4 Å for DQ. The diffusion constants D_i were calculated using the Stokes–Einstein equation ($\eta_{\text{heptane}}(25^\circ\text{C}) = 0.397 \text{ cp}$) [34]. The experimental rate constant is slightly smaller since the diffusion coefficient of the fluorophore/quencher pair in the excited state is smaller than the sum of ground state diffusion coefficients used to calculate the rate constant from Eq. (3) [37]. Therefore, it is possible to assume that the quenching process in *n*-heptane is diffusion controlled.

The contribution due to the active sphere of quenching and to the transient term Y can be estimated by fitting of Eq. (1)

to the experimental values of the emission intensities ratio (I_f^0/I_f), introducing the dynamic data (τ_f^0/τ_f) and the $\varepsilon_r K_C$ product obtained from the absorption data. In *n*-heptane, it was found that $R' = 9 \text{ \AA}$ and $D' = 1.3 \times 10^{-9} \text{ m}^2 \text{ s}^{-1}$, in reasonable agreement with reported literature data for similar systems [38]. The values of K_C , R' and D' are recorded in Table 1 and the good fitting obtained is shown in Fig. 2, respectively.

The fluorescence quenching of ZnTPP by DQ in ethylene glycol could not be detected possibly due to the low solubility of duroquinone in this solvent.

3.3. Fluorescence quenching $^1\text{ZnTPP}^*$ in *n*-heptane/AOT/Et Gly

The quenching of $^1\text{ZnTPP}^*$ by DQ in *n*-heptane/AOT/Et Gly resembles that observed in pure *n*-heptane. An upward curvature in the Stern–Volmer plot was also obtained for the different e_o molar ratios and is again interpreted as due to the contribution of both transient effects and excited state static quenching in these reverse micelles. There is an absorbance decrease of the Q and the Soret bands of ZnTPP in microemulsions. However, no red shift was observed in these media when the quencher concentration was increased. The isosbestic point was not so well defined as in the pure solvent. Besides, the decrease of the absorbance was smaller when a larger quantity of ethylene glycol was added to the micellar system.

Table 1

Association constant K_c (M^{-1}), lifetimes τ_f (ns), quenching rate constants k_q ($\text{mol dm}^{-3} \text{s}^{-1}$), effective distances R' (\AA) and diffusion coefficients ($\text{m}^2 \text{s}^{-1}$) values for *n*-heptane and *n*-heptane/AOT/ethylene glycol microemulsions

Medium	K_c^a	τ_f^b	τ_2^b	$k_{q1}/10^{10}$	$k_{q1}^o/10^{10}$	$k_{q2}/10^9$	$k_{q2}^e/10^9$	R'^c	$D'_o/10^{-9c}$	R_e^c	$D'_e/10^{-9c}$
<i>n</i> -Heptane	7.9	2.1	–	0.94	–	–	–	–	–	–	–
$e_o = 0$	7.9	2.0	2.9	1.10	1.21	4.72	1.72	9.5	1.3	11.5	0.5
$e_o = 1$	–	1.9	2.3	1.06	1.30	4.80	1.25	9.0	1.5	12.0	0.6
$e_o = 2$	–	1.8	2.3	1.11	1.37	4.70	0.76	9.0	1.5	11.5	0.6

^a Absorption data.

^b See [23].

^c Steady-state fluorescence (Eq. (1)).

The curvature plot of (I_f^o/I_f) versus the [DQ] decreases with the increase of the concentration of ethylene glycol in the medium, that is, by the increase of the molar ratio e_o (see Fig. 2) because the ground state complexation ZnTPP–DQ decreases when the ZnTPP resides at the interface and the majority of DQ is in the organic pseudophase.

Singlet state transient data is also shown in Fig. 2. Biexponential decays were obtained for all the molar ratios e_o studied and for all the quencher concentrations used. This behaviour confirms the presence of only two spectroscopically different species of ZnTPP, located at different zones of the reverse micelle (the organic pseudo-phase and the interface) as was shown in a previous work [23].

The k_q rate constant values obtained for the different molar ratios e_o from the transient measurements, using the Stern–Volmer equation for the lifetimes (Eq. (2)), are recorded in Table 1. As can be seen, the values of k_{q1} which correspond to the quenching of $^1\text{ZnTPP}^*$ molecules by DQ, both located in the organic bulk of the aggregate, are practically independent of the molar ratio e_o . The values do not differ much to that of pure *n*-heptane. Therefore, the quenching that takes place in the apolar environment of the microemulsion is diffusion-controlled, as it happens in the pure solvent (see above).

Taking into account that no quenching can be observed in ethylene glycol and this non-aqueous polar solvent is mainly located in the inner pool of the microemulsion, but close to the ionic head group of the surfactant as suggested earlier [23], the k_{q2} values must correspond to the quenching of the $^1\text{ZnTPP}^*$ molecules located at the interface and solvated by the ethylene glycol. We have compared these latter values to the k_q^{calc} (using Eq. (3)) in pure ethylene glycol, that is, $(3.9\text{--}4.8) \times 10^8 \text{ mol}^{-1} \text{ dm}^3 \text{ s}^{-1}$ (depending on the radii of ZnTPP and DQ used as happened in *n*-heptane). The values of k_{q2} quenching rate constant, which takes place in the interface, are one-order of magnitude higher than that calculated for ethylene glycol and, contrary to the expectations, they are also practically independent from the molar ratio e_o . This behaviour is anomalous and perhaps derives from the fact that only duroquinone molecules which reach the interface are able to quench the $^1\text{ZnTPP}^*$ molecules residing there.

Duroquinone is very soluble in the oil (*n*-heptane), but can solubilise partially in ethylene glycol, near to the inter-

face, and the quencher concentration in each region must be known. Assuming that the total absorbance is the sum of DQ absorbances in each pseudophase, Eq. (4) leads to the local concentrations.

$$A_{\text{total}}^{\text{DQ}} = A_o^{\text{DQ}} + A_e^{\text{DQ}} = \varepsilon_o^{\text{DQ}} [\text{DQ}_o] + \varepsilon_e^{\text{DQ}} [\text{DQ}_e] \quad (4)$$

where the different parameters are referred to the quencher located at the ethylene glycol (subscript e) or the *n*-heptane bulk (subscript o). The $\varepsilon_o^{\text{DQ}}$ can be directly measured from the spectrum of DQ in pure *n*-heptane, assuming that the microemulsion does not produce any effect on the quencher spectrum, located at the organic bulk. In order to determine $\varepsilon_o^{\text{DQ}}$ the absorption spectra of DQ in *n*-heptane/AOT/ethylene glycol microemulsions at different AOT concentrations ($0.025\text{--}0.45 \text{ mol dm}^{-3}$) and different molar ratios e_o ($e_o = 0, 1$ and 2) were recorded. The spectrum showed two peaks at 255.5 and 264 nm both in *n*-heptane and in the microemulsion [AOT] = $0.025 \text{ mol dm}^{-3}$. At all the molar ratios studied the maximum absorption (A_{max}) of the two peaks decrease when the AOT concentration increases reaching a plateau at high surfactant concentrations.

A plot of A_{max} versus [AOT] shows a plateau of the absorption, which should correspond to a system where all the quencher resides at the interface, enabling the calculation of the molar extinction coefficient $\varepsilon_e^{\text{DQ}}$. The values obtained are the following: $\varepsilon_o^{\text{DQ}}$ (255.5 nm) = $18463 \text{ mol}^{-1} \text{ dm}^3 \text{ cm}^{-1}$, $\varepsilon_o^{\text{DQ}}$ (264 nm) = $18443 \text{ mol}^{-1} \text{ dm}^3 \text{ cm}^{-1}$, $\varepsilon_e^{\text{DQ}}$ (255.5 nm) = $14998 \text{ mol}^{-1} \text{ dm}^3 \text{ cm}^{-1}$ and $\varepsilon_e^{\text{DQ}}$ (264 nm) = $16018 \text{ mol}^{-1} \text{ dm}^3 \text{ cm}^{-1}$. The concentration ratio obtained was $[\text{DQ}_o]/[\text{DQ}_e] \cong 3$ for all the molar ratios, enabling the calculation of the effective concentrations at each pseudophase, $[\text{DQ}_o]_i$, in the oil and at ethylene glycol/interface, $[\text{DQ}_e]_i$. The latter was estimated assuming a spherical shell determined from the hydrodynamic radii previously found for this system [13].

In Fig. 3 are given the Stern–Volmer plots assuming that each spectroscopic species of $^1\text{ZnTPP}^*$ is quenched only by the quencher located at the oil or at the interface, respectively. The rate constants extracted from Fig. 3 are also shown in Table 1 and the comparison with those obtained using the quencher analytical concentration shows that whereas the k_{q1}^o hardly changes, the k_{q2}^e are now much lower and decrease with the increase of molar ratio e_o , but

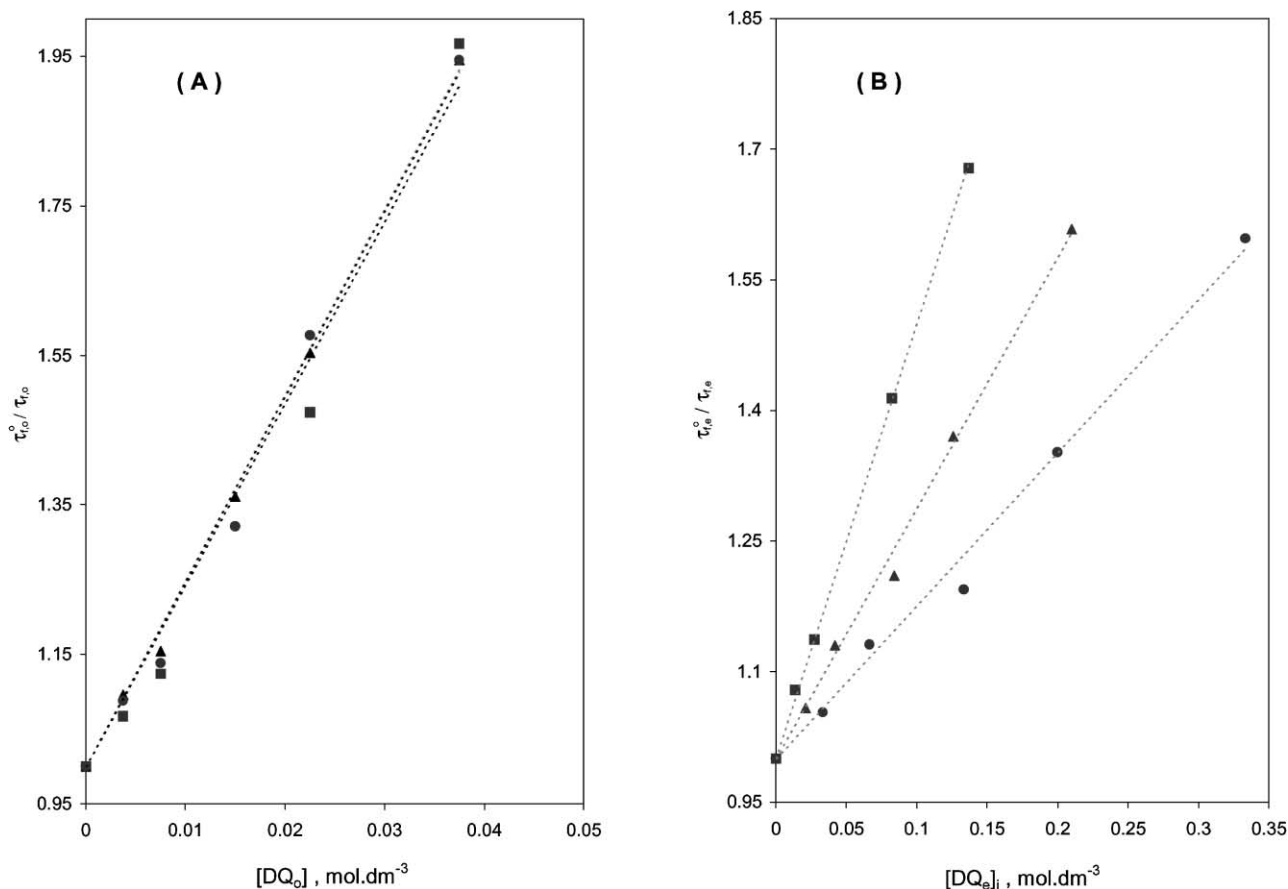


Fig. 3. (A) Correlation of the $(\tau_{f,o}^0/\tau_{f,o})$ vs. the $[DQ_o]$ (see text); (B) correlation of $\tau_{f,e}^0/\tau_{f,e}$ vs. $[DQ_e]_i$ (see text) at $e_o = 0$ (■); $e_o = 1$ (▲); and $e_o = 2$ (●).

are still higher than the diffusion control limit in ethylene glycol. In $e_o = 2$, the corresponding rate constant is two times the value in pure ethylene glycol.

The steady-state curves can be adjusted (Fig. 2) using the linear correlation of lifetimes at the oil and at the interface, the transient term Y and the exponential static term in Eq. (1) by fitting parameters R' and D' . The ground state association was neglected for $e_o = 1$ and 2. The best values obtained for R' and D' are shown in Table 1. It is clear that R' increases and D' decrease at the interface. The diffusion limit can then be recalculated using Eq. (3) and the value of the bimolecular diffusion controlled rate at the interface is around $4.35 \times 10^9 \text{ mol}^{-1} \text{ dm}^3 \text{ s}^{-1}$. Thus, the k_{q2}^e values obtained are near diffusion-controlled at $e_o = 0$ and lower at higher molar ratio perhaps due to a mutual orientation factor of approach of both species fluorophore and quencher.

3.4. T - T spectra of ZnTPP in n -heptane/AOT/Et Gly microemulsions

Laser photoexcitation of ZnTPP in n -heptane/AOT/Et Gly microemulsions produces the transient absorption spectra shown in Fig. 4, for the molar ratios $e_o = 0, 1$ and 2. In all cases, the absorption maxima for the triplet state $^3\text{ZnTPP}^*$

is located around 460–470 nm, as it has been previously described in the literature. Fig. 4 shows the absorption spectra for the different molar ratios $[\text{EtGly}]/[\text{AOT}]$ studied in the present work in the wavelength range 380–550 nm and,

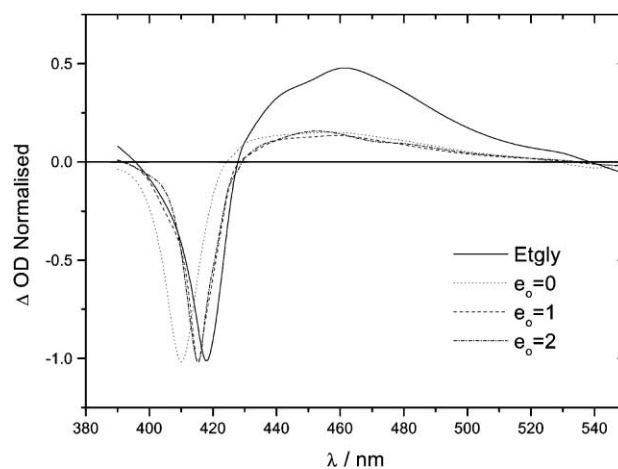


Fig. 4. Normalised T - T absorption spectra of ZnTPP in n -heptane/AOT/ethylene glycol and ethylene glycol at different molar ratios e_o after the laser flash.

for comparison purposes, also the triplet–triplet spectra of ZnTPP in ethylene glycol. A clear red shift of the Soret band is observed when e_o increases which does not reach the value in the bulk liquid. For $e_o = 1$, a small shoulder of the band is also seen which can be due to ZnTPP molecules located in the polar solvent of the aggregates. Therefore, laser flash photolysis measurements seem to confirm the displacement of porphyrin molecules from the organic phase to the interface as shown previously from absorption and emission spectroscopy [23].

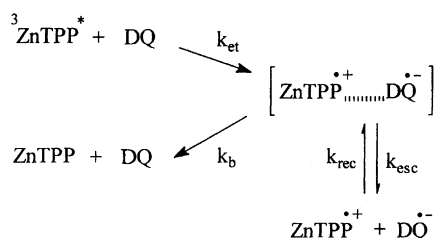
The triplet decay lifetime, τ_T^o , in *n*-heptane is monoexponential, but in ethylene glycol the decay does not adjust completely to a monoexponential ($\tau_T^e \sim 2$ ms) and a very small amount of a second component (~ 200 μ s) was detected.

Biexponential decays were clearly observed in all the microemulsions, but the contribution of the short species decreases from $e_o = 0$ to 2 (Table 2).

3.5. Ion radicals formation in *n*-heptane/AOT/Et Gly

3.5.1. ZnTPP/DQ

The quinone DQ is very soluble in *n*-heptane and almost insoluble in ethylene glycol. Therefore, in microemulsions the quenching should take place in the apolar organic phase, but as the molar ratio e_o is increased a contribution of duroquinone molecules at the interface has to be taken into account. Addition of different concentrations of duroquinone produces a decrease of the τ_T values due to the electron transfer reaction which takes place between the triplet excited ZnTPP molecules and the quencher (see Table 2) [25,30] followed by recombination of the ion radicals formed:



At the organic pseudophase $k_b \gg k_{\text{esc}}$ since the radical ions are not well solvated in this medium. Both lifetimes are quenched which means that the interaction in the two pseudophases is possible as also happened in the

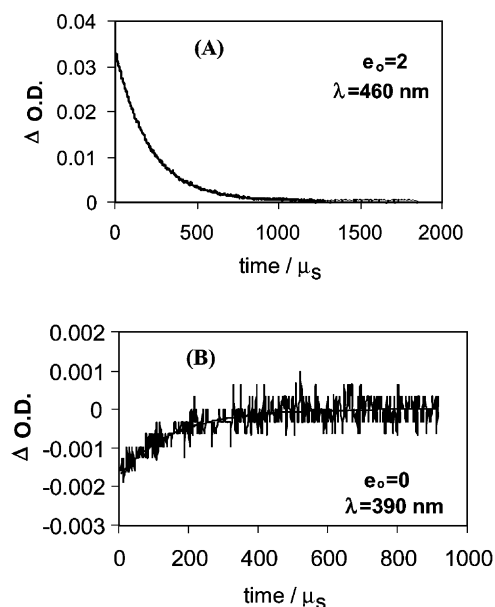


Fig. 5. Variation of the optical density of ${}^3\text{ZnTPP}^*$ following a laser flash in *n*-heptane/AOT/ethylene glycol at different wavelengths and molar ratios e_o : (A) $\lambda = 460$ nm and $e_o = 2$; (B) $\lambda = 390$ nm and $e_o = 0$. Line represents the best fitting of the decays obtained.

singlet excited state, which is likely related to the different locations of such molecules in the non-aqueous microemulsions.

When no ethylene glycol is added to the medium, that is at the molar ratio $e_o = 0$ (Fig. 5), although the triplet is quenched no radical ions are observed due to the apolar bulk of the micellar system where electron transfer processes (k_{et}), escape (k_{esc}), recombination (k_{rec}) and back electron transfer (k_b) can occur. When ethylene glycol is added to the system, a displacement of ZnTPP molecules takes place in a more polar environment where the ion radicals can exist separately. It is worth pointing out the presence of the radical cation $\text{ZnTPP}^{\bullet+}$, and the radical anion $\text{DQ}^{\bullet-}$ at 405 and 428 nm, respectively, at the molar ratios $e_o = 1$ and 2 (see Fig. 6). Besides, it was noticed that the absorbance of radical ions are higher at $e_o = 2$ than at 1 for the same ZnTPP and DQ concentrations, likely because ${}^3\text{ZnTPP}^*$ molecules are mainly located at the interface at $e_o = 2$ while they are distributed between the organic bulk and the interface at $e_o = 1$, as was confirmed by the transient absorption spectra.

Table 2

Lifetimes τ_T^o (μ s) and τ_T^e (μ s), intrinsic decay rate constants k_D^o (μs^{-1}) and k_D^e (μs^{-1}) and triplet quenching rate constants k_q^o , k_q^e , k_q^T and k_2 ($\text{mol}^{-1} \text{dm}^3 \text{s}^{-1}$)

Medium	τ_T^o	$1/k_D^o$	τ_T^e	$1/k_D^e$	$k_q^o/10^9$	$k_q^e/10^8$	$k_q^T/10^6$	$k_2/10^8$
<i>n</i> -Heptane	80	48.5	–	–	5.86	–	–	–
Et Gly	–	–	2056	2057.6	–	7.09	–	–
$e_o = 0$	98	78.1	330	190	5.52	2.37	–	–
$e_o = 1$	80	12.2	340	228	10.9	1.86	–	–
$e_o = 2$	62.6	38.5	218	147	6.78	0.87	2.1 ^a	4.2 ^b

^a Quencher MV^{2+} ; forward rate constant.

^b Quencher MV^{2+} ; back electron transfer rate constant.

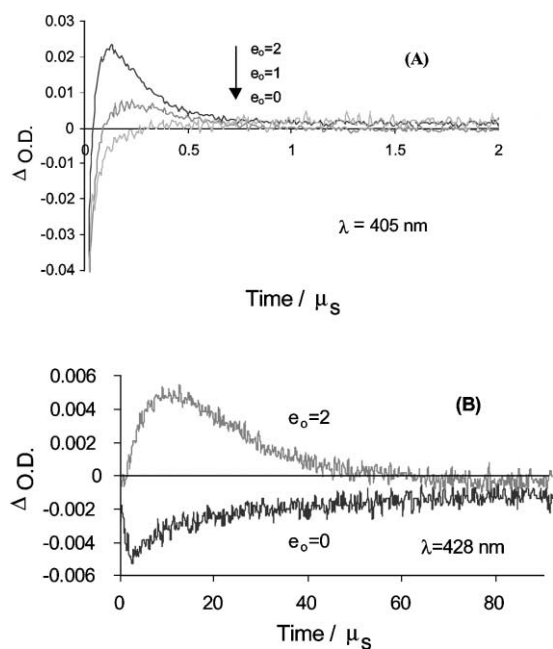


Fig. 6. Variation of the optical density of radical ions at (A) $\lambda = 405$ nm ($\text{ZnTPP}^{\bullet+}$) and (B) $\lambda = 428$ nm ($\text{DQ}^{\bullet-}$) following a laser flash in *n*-heptane/AOT/ethylene glycol at different e_o values.

The shortening of the triplet lifetime upon increasing the concentration of duroquinone can be rationalised in terms of a diffusional electron-transfer quenching of the $^3\text{ZnTPP}^*$ to the electron acceptor DQ.

According to this, the time-dependent concentration decay of the triplet state, $^3\text{ZnTPP}^*$, is given by the following equations:

$$[{}^3\text{ZnTPP}_o^*](t) = [{}^3\text{ZnTPP}_o^*](0) \exp(-k_{\text{obs}}^o t),$$

where $k_{\text{obs}}^o = k_D^o + k_q^o[\text{DQ}_o]$ (5a)

$$[{}^3\text{ZnTPP}_e^*](t) = [{}^3\text{ZnTPP}_e^*](0) \exp(-k_{\text{obs}}^e t),$$

where $k_{\text{obs}}^e = k_D^e + k_q^e[\text{DQ}_e]$ (5b)

the subscripts o and e represent the *n*-heptane bulk and the interface where the ethylene glycol molecules are found [13], respectively. The quencher concentrations were calculated in the same way as referred earlier and depicted in Fig. 4. The k_{obs}^o and k_{obs}^e are the observed rate constants of the processes, which take place in the organic bulk (o) and the interface (e) of the reverse micelles at each quencher concentration added. k_D and k_q are, respectively, the intrinsic decay constants of $^3\text{ZnTPP}^*$ and the quenching electron transfer rate constants of $^3\text{ZnTPP}^*$ by the electron acceptor DQ.

From Eqs. (5a) and (5b), k_q^o , k_q^e , k_D^o and k_D^e can be obtained from the slope and intercept of the linear correlation between k_{obs} versus $[\text{DQ}]$ for each pseudophase.

Stern–Volmer relationships are found between the reciprocal lifetimes of each $1/\tau_T^o$ and $1/\tau_T^e$ versus the local quencher concentrations $[\text{DQ}_o]$ and $[\text{DQ}_e]$, where τ_T^o and

τ_T^e are the lifetimes of $^3\text{ZnTPP}^*$ located at the *n*-heptane bulk and the interface, respectively (see Fig. 7A and B). The kinetic data obtained are recorded in Table 2 where it can be observed that triplet intrinsic decay rate constants, k_D^o and k_D^e extracted are within the expected order of magnitude.

As can be seen, the results are in accordance with those for the singlet state: the electron-transfer rate quenching of the process that takes place in the organic bulk has a value comparable to that in pure *n*-heptane, while the electron transfer rate quenching k_q^e of the reaction which takes place in the interface of the microemulsion decreases with the molar ratio e_o , reaching values nearly one-order of magnitude smaller than in pure ethylene glycol. This may be due to larger microviscosities at the interface and restricted geometry which are felt at this time scale. In a similar type of AOT microemulsions of glycerol, the microviscosities calculated from steady-state fluorescence anisotropy parameters determined experimentally increase with the molar ratio $g_o = [\text{Gly}]/[\text{AOT}]$. By contrast, in AOT aqueous microemulsions the microviscosities determined in the same way decrease with the increase of $w_o = [\text{H}_2\text{O}]/[\text{AOT}]$ [39]. The values of diffusion coefficients extracted from the singlet state quenching lead also to the conclusion that the microviscosities in ethylene glycol at the interface are greater than the bulk solvent viscosity.

3.5.2. ZnTPP/methyl viologen

This quencher is not soluble in *n*-heptane, but it is very soluble in ethylene glycol and, therefore, it will be expected that the molecules inside the pool can interact with the ZnTPP triplet that is solvated by the ethylene glycol.

The transient difference absorption spectra at $e_o = 1$ show the quenching of the triplet state at 470 nm with the appearance of a growing at 400 nm which can be attributed to both $\text{ZnTPP}^{\bullet+}$ and $\text{MV}^{\bullet+}$ at 405 and 395 nm, respectively, according to the well known electron transfer process [25] (Fig. 8). Interestingly, the ion radicals in this system live long enough to be detected, whereas when the donor species is Zinc meso-tetrakis(*n*-methylpyridinium)porphyrin and the acceptor is also MV^{2+} in AOT aqueous microemulsions the quenching process occurs, but the recombination is very fast and it is not possible to detect radical ions [40].

A biexponential decay at 470 nm where the triplet absorbs shows that only one species suffers the quenching process either at $e_o = 1$ or 2 using MV^{2+} in a local concentration range of (0–0.15) M referred to the pool volume [41].

Considering the initial electron transfer, the back reaction and the triplet intrinsic decay:



a global analysis was carried out for the decays obtained at 470, 405 and 395 nm for the microemulsion $e_o = 2$ with a

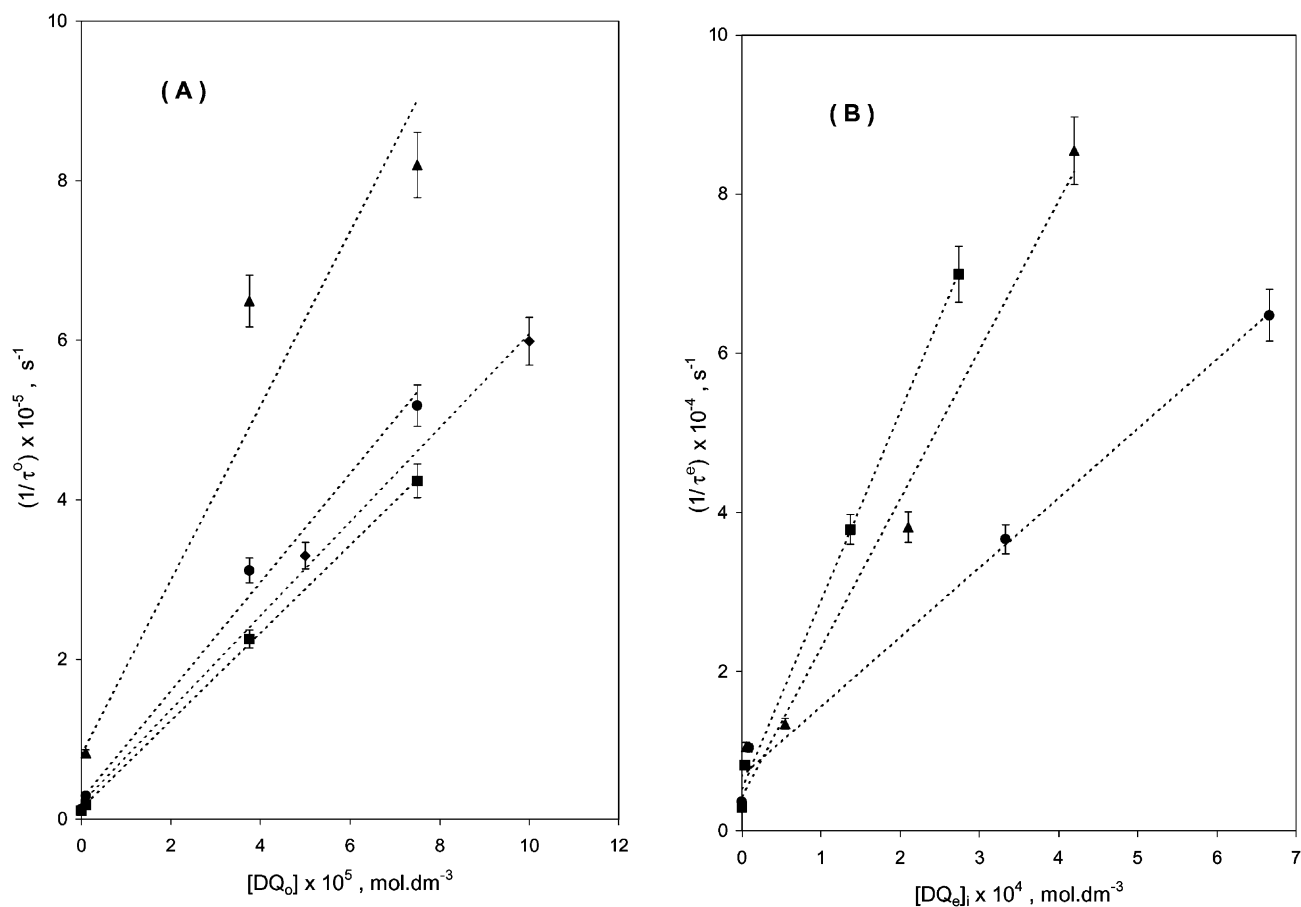


Fig. 7. Correlation of the reciprocal triplet lifetimes (A) in oil vs. $[\text{DQ}_o]$, (B) at the interface vs. $[\text{DQ}_e]$; (see text) for n -heptane (\blacklozenge); $\epsilon_o = 0$ (\blacksquare); $\epsilon_o = 1$ (\blacktriangle); and $\epsilon_o = 2$ (\bullet).

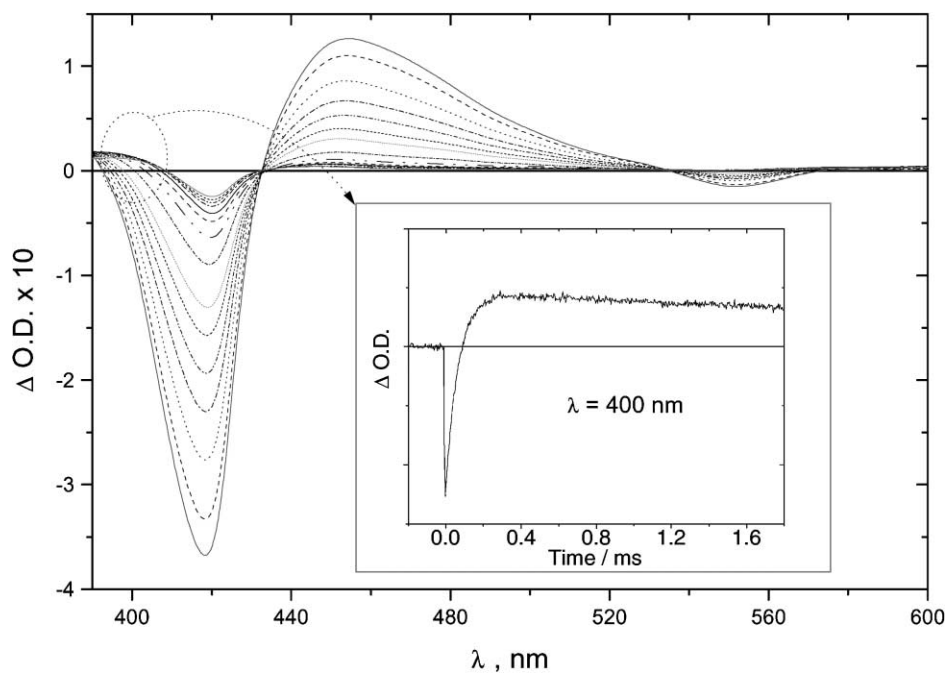


Fig. 8. Difference transient absorption spectra of $^3\text{ZnTPP}^*$ in n -heptane/AOT/ethylene glycol at $\epsilon_o = 1$ with $[\text{MV}^{2+}] = 4.5 \times 10^{-4} \text{ mol dm}^{-3}$. Inset: growing of MV^{*+} and ZnTPP^{*+} at $\lambda = 400 \text{ nm}$.

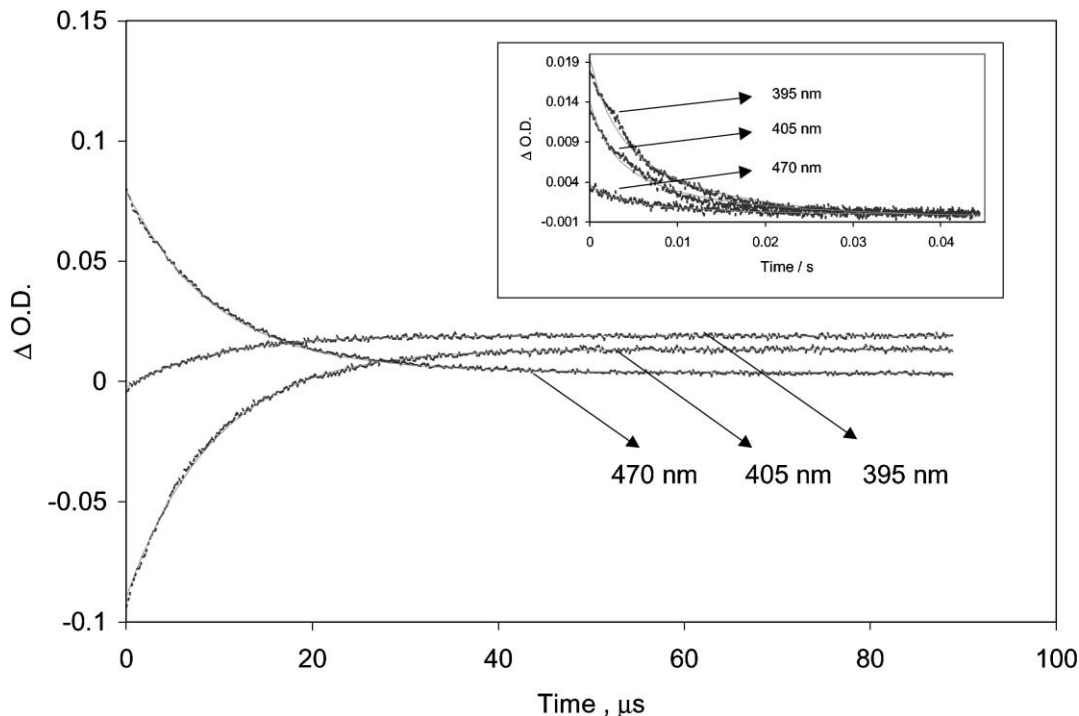


Fig. 9. Fitting of decays at different wavelengths using equations (see text) (6a–c). Inset: the same decays at different time scale.

local concentration of $[MV^{2+}] = 5.03 \times 10^{-2}$ M (Fig. 9), using the multiple exponentials Eqs. (6a)–(6c), which account approximately for the intrinsic decay (k_0^T), the forward electron transfer (k_q^T) and back electron transfer (k_2). The experimental differential absorption at each wavelength λ is composed by the short lifetime component ΔOD_s^λ and long lifetime component ΔOD_l^λ .

$$\Delta OD_{\text{exp}}^\lambda = \Delta OD_s^\lambda + \Delta OD_l^\lambda \quad (6a)$$

In the short time scale the most representative species are the ZnTPP triplet decay and the growing of radical ions originated from the triplet electron transfer quenching by methyl viologen with rate constant k_q^T . Both processes were globally fitted by:

$$\begin{aligned} \Delta OD_s^\lambda &= \Delta OD_{t=0}^\lambda \exp\{-(k_0^T + k_q^T[MV^{2+}])t\} \\ &+ \Delta OD_{t=\infty}^\lambda \{1 - \exp\{-(k_0^T + k_q^T[MV^{2+}])t\}\} \end{aligned} \quad (6b)$$

In Eq. (6b), $\Delta OD_{t=0}^\lambda$ and $\Delta OD_{t=\infty}^\lambda$ are the differential absorptions at time zero and long time value which are proportional to the triplet and ions radical concentrations, respectively. The value for the intrinsic triplet decay, k_0^T , is an average one since the ZnTPP triplet is not monoexponential in these microemulsions. At long time scale, the decays were fitted using the second order kinetic expression:

$$\Delta OD_l^\lambda = \frac{\Delta OD_{t=\infty}^\lambda}{1 + \Delta OD_{t=\infty}^\lambda (k_2 / \delta \varepsilon^\lambda) t} \quad (6c)$$

where $\delta \varepsilon^\lambda = (\varepsilon_{\text{ion radicals}}^\lambda - \varepsilon_{\text{ZnTPP}}^\lambda)l$ is the difference between the molar absorptivity coefficients of ion radicals and the ZnTPP at wavelength λ by path l (around 1 cm).

The fittings were good (Fig. 9) and the value of the rate constant evaluated for the forward electron transfer is $k_q^T = 2.1 \times 10^6 \text{ mol}^{-1} \text{ dm}^3 \text{ s}^{-1}$ showing, that in this case, the process is reaction controlled (see Table 2). Considering an absorptivity $\varepsilon_{MV^{\bullet+}}^{395} \gg \varepsilon_{ZnTPP}^{395}$ and $\delta \varepsilon^{395} \approx \varepsilon_{MV^{\bullet+}}^{395} = 4.1 \times 10^4 \text{ mol}^{-1} \text{ dm}^3 \text{ cm}^{-1}$ [42], the bimolecular rate constant for the ion radicals recombination is $k_2 = 4.2 \times 10^8 \text{ mol}^{-1} \text{ dm}^3 \text{ s}^{-1}$, a value very close to the diffusion control rate constant in ethylene glycol (Table 2).

4. Final remarks

In the microheterogeneous systems of nonaqueous microemulsions it is possible to follow both kinetic and spectroscopically the formation of radical ions originated from an electron transfer process. If the donor excited species can be located in either side at the interface with respectively apolar and polar microvicinities, the use of different acceptors placed either in the organic apolar pseudophase or in the pool can afford different kinetic features related, respectively, to diffusion controlled or reaction control processes.

The ensemble of data were obtained from two different spectroscopic techniques and are also consistent with those obtained in a previous work [17]: in this type of systems, the porphyrin is displaced from the organic bulk to the polar

phase when ethylene glycol is added to the medium and participates in bimolecular reactions from either side of the interface.

The accurate determination of solute partition as well as the evaluation of changes in the microscopic physical properties (polarity and viscosity) which can be assessed by fluorescence quenching techniques in these aggregates are of fundamental importance for studies dealing with these new microemulsions, which can be viewed as mimetic microreactors of relevance for polymerisation reactions.

Acknowledgements

The authors acknowledge the financial support of the project PRAXIS 2/2.1/QUI/443/94 and Dr. P.P. Levin for the initial collaboration in the Laser Flash Photolysis experiments. P. López-Cornejo thanks the Ayuda a Proyectos de Investigación para Grupos Precompetitivos (Plan Propio de la Universidad de Sevilla). D.M. Togashi acknowledges a BPD/16345 grant from FCT/PRAXIS XXI and C.A.T. Laia acknowledges a Ph.D. Grant BD no 961 from Praxis XXI.

References

- [1] J. Fendler, *Acc. Chem. Res.* 10 (1980) 133.
- [2] K. Kalyanasundaram, *Photochemistry in Microheterogeneous Systems*, Academic Press, Orlando, 1987.
- [3] M. Wong, J.K. Thomas, T. Nowak, *J. Am. Chem. Soc.* 99 (1977) 4730.
- [4] R.F. Berg, M.R. Moldover, J.S. Huang, *J. Chem. Phys.* 87 (1987) 3687.
- [5] R. Jiménez, M.M. Graciani, A. Rodríguez, M.L. Moyá, F. Sánchez, P. López-Cornejo, *Langmuir* 13 (1997) 187.
- [6] B.H. Robinson, D.C. Steytler, R.D. Tack, *J. Chem. Soc., Faraday Trans.* 75 (1979) 132.
- [7] B.H. Robinson, C. Toprakcioglu, J.C. Dore, P. Chieux, *J. Chem. Soc., Faraday Trans.* I 80 (1984) 13.
- [8] C. Toprakcioglu, J.C. Dore, B.H. Robinson, A. Howe, P. Chieux, *J. Chem. Soc., Faraday Trans.* I 80 (1984) 413.
- [9] R.A. Day, B.H. Robinson, J.H.R. Doherty, *J. Chem. Soc., Faraday Trans.* 1 75 (1979) 132.
- [10] J.M. Furois, P. Brochette, M.P. Pileni, *J. Colloid Int. Sci.* 97 (1984) 552.
- [11] P. Brochette, T. Zemb, P. Mathis, M.P. Pileni, *J. Phys. Chem.* 91 (1987) 1444.
- [12] C. Izquierdo, M.L. Moyá, J.L. Usero, J. Casado, *Monatsh. Chem.* 123 (1992) 383.
- [13] C.A.T. Laia, P. López-Cornejo, S.M.B. Costa, J. d'Oliveira, J.M.G. Martinho, *Langmuir* 14 (1998) 3531.
- [14] C.A.T. Laia, W. Brown, M. Almgren, S.M.B. Costa, *Langmuir* 16 (2000) 8763.
- [15] R.E. Riter, E.P. Undikis, N.E. Levinger, *J. Phys. Chem. B* 102 (1998) 7931.
- [16] E. Geladé, N. Boens, F.C. De Schryver, *J. Am. Chem. Soc.* 104 (1982) 6288.
- [17] S.M.B. Costa, M.R. Aires, J.P. Conde, *J. Photochem.* 28 (1985) 153.
- [18] S.M.B. Costa, R.L. Brookfield, *J. Chem. Soc., Faraday Trans.* 2 82 (1986) 991.
- [19] S.M.B. Costa, M.M. Velázquez, N. Tamai, I. Yamazaki, *J. Luminescence* 48/49 (1991) 341.
- [20] A. Harriman, G. Porter, N. Searle, *J. Chem. Soc., Faraday Trans.* 2 75 (1979) 1515.
- [21] D. Gust, T.A. Moore, A.L. Moore, *Acc. Chem. Res.* 26 (1993) 198.
- [22] M.R. Wasielewski, *Chem. Rev.* 92 (1992) 435.
- [23] P. López-Cornejo, S.M.B. Costa, *Langmuir* 14 (1998) 2042.
- [24] D.M. Togashi, S.M.B. Costa, *Phys. Chem. Chem. Phys.* 2 (2000) 5437.
- [25] P.J.G. Coutinho, S.M.B. Costa, *J. Photochem. Photobiol. A: Chem.* 82 (1994) 149.
- [26] F.M. Menger, *J. Am. Chem. Soc.* 101 (1979) 6732.
- [27] D.V. O'Connor, D. Phillips, In *Time Correlated Single Photon Counting*, Academic Press, London, 1984, p. 1333.
- [28] D.W.J. Marquardt, *J. Soc. Ind. Appl. Math.* 11 (1963) 431.
- [29] P.J.G. Coutinho, S.M.B. Costa, *Chem. Phys.* 182 (1994) 399.
- [30] S.E. Webber, *Photochem. Photobiol.* 65 (1997) 33.
- [31] R.W. Larsen, R. Jasuja, S.-L. Niu, K. Dwivedi, *J. Photochem. Photobiol. A: Chem.* 107 (1997) 71.
- [32] F. Perrin, *Compt. Rend.* 178 (1924) 1978.
- [33] S.M.B. Costa, A.L. Maçanita, *J. Phys. Chem.* 84 (1980) 2408.
- [34] P.W. Atkins, *Physical Chemistry*, Fourth Edition, Oxford University Press, Oxford, 1990, p. 846.
- [35] F. Lendzian, B. von Maltzan, *Chem. Phys. Lett.* 180 (1991) 191.
- [36] M.D. Archer, V.P.Y. Gadzekpo, J.R. Bolton, J.A. Schmidt, A.C. Weedon, *J. Chem. Soc., Faraday Trans.* 2 82 (1986) 2305.
- [37] H. Saiki, K. Takami, T. Tominaga, *Phys. Chem. Chem. Phys.* 1 (1999) 303.
- [38] G.B. Dutt, N. Periasamy, *J. Chem. Soc., Faraday Trans.* 87 (1991) 3815.
- [39] C.A.T. Laia, S.M.B. Costa, submitted to *Langmuir*.
- [40] D.M. Togashi, unpublished results.
- [41] S.M.B. Costa, J.M.F.M. Lopes, M.J. Martins, *J. Chem. Soc., Faraday Trans.* 2 86 (1986) 2371.
- [42] T. Wanatabe, K. Honda, *J. Phys. Chem.* 86 (1982) 2617.